

# SUPPLEMENTAL MATERIAL

## Targeting Interleukin-1 $\beta$ reduces leukocyte production after acute myocardial infarction

Hendrik B. Sager<sup>1\*</sup>, MD, Timo Heidt<sup>1\*</sup>, MD, Maarten Hulsmans<sup>1</sup>, PhD, Partha Dutta<sup>1</sup>, DVM, PhD, Gabriel Courties<sup>1</sup>, PhD, Matthew Sebas<sup>1</sup>, BA, Gregory R. Wojtkiewicz<sup>1</sup>, MSc, Benoit Tricot<sup>1</sup>, MSc, Yoshiko Iwamoto<sup>1</sup>, BA, Yuan Sun<sup>1</sup>, MD, PhD, Ralph Weissleder<sup>1,2</sup>, MD, PhD, Peter Libby<sup>3</sup>, MD, Filip K. Swirski<sup>1</sup>, PhD, Matthias Nahrendorf<sup>1</sup>, MD, PhD

<sup>1</sup>Center for Systems Biology, Massachusetts General Hospital and Harvard Medical School, Simches Research Building, 185 Cambridge St., Boston, MA 02114, USA; <sup>2</sup>Department of Systems Biology, Harvard Medical School; <sup>3</sup>Cardiovascular Division, Department of Medicine, Brigham and Women's Hospital, Boston, MA, USA.

## Supplemental Methods

**Experimental animals.** We used female C57BL/6J (WT, n=162), B6.129S7-Il1r1tm1Imx/J (IL1R1<sup>-/-</sup>, n=28 and apolipoprotein E-deficient (ApoE<sup>-/-</sup>; B6.129P2-Apoetm1Unc/J, n=24) mice aged 8-12 weeks (The Jackson Laboratories, Bar Harbor, ME, USA) for our studies. We also used transgenic mice expressing green fluorescent protein (GFP) under the Nestin-promoter (Nestin-GFP, n=10)<sup>1, 2</sup>. Nestin-GFP mice were a gift from Dr. Grigori Enikolopov (Cold Spring Harbor Laboratory, NY, USA). Nestin-GFP were crossed to C57B6 mice for at least 8 generations. Age-matched mice were randomly allocated either to control or treatment groups. The study was approved by the Subcommittee on Animal Research Care at Massachusetts General Hospital (Boston, MA).

**Myocardial infarction surgery.** Myocardial infarction was induced by permanent ligation of the left anterior descending coronary artery as described previously<sup>3</sup>. Mice were anesthetized with 2% isoflurane (with O<sub>2</sub> 2 l/min), intubated and ventilated. All mice scheduled for infarct surgeries were injected twice daily with buprenorphine (0.1 mg/kg i.p.) for three days, starting on the day of the surgery.

**Ischemia Reperfusion Injury** was induced and assessed as described previously<sup>4</sup>. In brief, we ligated the the left anterior descending coronary artery and injected 360,000 fluorescent microspheres (10 μm size, excitation/emission wavelength 580/605 nm, Invitrogen) into the left ventricle 5 min thereafter. After 35 min of ischemia we released the suture waited for another 10 min and then injected 10 mg/kg bodyweight of the IL-1β antibody (or a mouse monoclonal IgG2a antibody raised against cyclosporine A as isotype control). Twenty-four hours after the induction of the ischemia, we conducted 2,3,5-triphenyltetrazolium chloride (TTC, Sigma-Aldrich, St. Louis, MO, USA) staining to evaluate myocardial necrosis and fluorescence reflectance imaging (FRI) to quantify the ischemic area at risk (OV110, Olympus).

**Parabiosis.** Mice were joined in parabiosis as described perviously<sup>5</sup>. Mice were anesthetized with 2% isoflurane (with O<sub>2</sub> 2 l/min). All mice scheduled for parabiosis surgeries were injected twice daily with buprenophine (0.1 mg/kg i.p.) for three days, starting on the day of the surgery.

**Neutralizing IL-1 $\beta$ .** The IL-1 $\beta$  neutralizing antibody was a donation from Novartis (Basel, Switzerland). The antibody selectively binds IL-1 $\beta$ , thus blocking the interaction of the cytokine with its receptors. We used a monoclonal, mouse anti-mouse IL-1 $\beta$  IgG2a/k antibody derived from an IgG1/k antibody as described by Geiger et al.<sup>6</sup>. The in vitro potency IC<sub>50</sub> is about 25 pM, and its affinity to murine IL-1 $\beta$  is about 300 pM. The  $t_{1/2}$  in mice is 14 days<sup>7</sup>. We initiated treatment 2 h after induction of MI with subcutaneously injecting 10 mg/kg bodyweight of the IL-1 $\beta$  antibody (or a mouse monoclonal IgG2a antibody raised against cyclosporine A as isotype control). We repeated injections once weekly over the study period.

**Generating cell suspensions.** Blood for flow cytometric analysis was collected by cardiac puncture using a 50 mM EDTA (Ethylene diamine tetra acetic acid) solution (Sigma Aldrich, St. Louis, MO, USA) as an anticoagulant. Erythrocytes were lysed using a red blood cell lysis buffer (Biolegend, San Diego, CA, USA). After organ harvest, single-cell suspensions were obtained as follows. Hearts were extensively flushed with PBS and then removed. Infarct and border zone were separated from remote myocardium using a dissection microscope, minced with scissors and digested in collagenase I (450 U/ml), collagenase XI (125 U/ml), DNase I (60 U/ml) and hyaluronidase (60 U/ml) (Sigma-Aldrich, St. Louis, MO, USA) at 37° C at 750 rpm for 1 hour<sup>8,9</sup>. Hearts were then homogenized through a 40- $\mu$ m cell strainer. Bone marrow was flushed out from bones and homogenized through 40- $\mu$ m cell strainers. To sort stromal cells from the hematopoietic stem cell microenvironment, we harvested bones from nestin-GFP mice as described previously<sup>10</sup>. Bone marrow endothelial cells (EC) and mesenchymal stromal cells (MSC) were obtained by flushing out and subsequent digesting bone marrow in 10 mg/ml

collagenase type IV (Worthington) and 20 U/ml DNase I (Sigma). Bone osteoblastic lineage cells were obtained by crushing bones and washing off residual bone marrow cells. We then digested and incubated the bone fragments in collagenase IV and 20 U/ml DNase I as described above. Spleens were removed and then homogenized through a 40- $\mu$ m cell strainer. Total viable cell numbers were obtained using Trypan blue (Cellgro, Mediatech, Inc., VA, USA).

**Flow cytometry.** For myeloid cell staining, cell suspensions were stained with mouse hematopoietic lineage markers (lineage for myeloid staining) including phycoerythrin (PE) anti-mouse antibodies directed against B220 (BD Bioscience, clone RA3-6B2), CD90 (BD Bioscience, clone 53-2.1), CD49b (BD Bioscience, clone DX5), NK1.1 (BD Bioscience, clone PK136), Ly6G (BD Bioscience, clone 1A8) and Ter-119 (BD Bioscience, clone TER-119). We then applied a second round of staining covering CD45.2 (BD Bioscience, clone 104), CD11b (BD Bioscience, clone M1/70), CD115 (eBioscience, clone M1/70), CD11c (eBioscience, clone HL3), F4/80 (Biolegend, clone BM8) and Ly6C (BD Bioscience, clone AL-21). Neutrophils were identified as (B220/CD90/CD49b/NK1.1/Ly6G/Ter119)<sup>high</sup> (CD45.2/CD11b)<sup>high</sup> CD115<sup>low</sup>, monocytes as (B220/CD90/CD49b/NK1.1/Ly6G/Ter119)<sup>low</sup> (CD45.2/CD11b)<sup>high</sup> (F4/80/CD11c)<sup>low</sup> CD115<sup>high</sup> Ly6C<sup>high/low</sup> and macrophages as (B220/CD90/CD49b/NK1.1/Ly6G/Ter119)<sup>low</sup> (CD45.2/CD11b)<sup>high</sup> Ly6C<sup>low/int</sup> F4/80<sup>high</sup> 8, 9. For hematopoietic stem/progenitor staining, cell suspensions were incubated with biotin-conjugated anti-mouse antibodies (lineage for hematopoietic stem/progenitor staining) directed against B220 (eBioscience, clone RA3-6B2), CD11b (eBioscience, clone M1/70), CD11c (eBioscience, clone N418), NK1.1 (eBioscience, clone PK136), TER-119 (eBioscience, clone TER-119), Gr-1 (eBioscience, clone RB6-8C5), CD8a (eBioscience, clone 53-6.7), CD4 (eBioscience, clone GK1.5) and IL7R $\alpha$  (eBioscience, clone A7R34) followed by incubation with an anti-biotin pacific orange-conjugated streptavidin antibody. Cell suspensions were then stained with antibodies directed against c-kit (BD Bioscience, clone 2B8), sca-1 (eBioscience, clone D7) and SLAM markers CD48 (eBioscience, clone HM48-1) and CD150 (Biolegend, clone TC15-12F12.2). Hematopoietic Lin-

Sca-1<sup>+</sup> c-Kit<sup>+</sup> (LSK) were identified as (B220/CD11b/CD11c/NK1.1/Ter-119/Gr-1/CD8a/CD4/IL7R $\alpha$ )<sup>low</sup> c-kit<sup>high</sup> sca-1<sup>high</sup>, hematopoietic stem cells (HSC) as (B220/CD11b/CD11c/NK1.1/Ter-119/Gr-1/CD8a/CD4/IL7R $\alpha$ )<sup>low</sup> c-kit<sup>high</sup> sca-1<sup>high</sup> CD48<sup>low</sup> CD150<sup>high</sup>. We acquired data on an LSRII flow cytometer (BD Bioscience) with FACSDiva software (BD Bioscience). Experimental data were later analyzed using FlowJo software (Tree Star Inc.).

**BrdU incorporation experiments.** To assess proliferation, we used FITC/APC BrdU (bromodeoxyuridine) flow kits (BD Bioscience). For these BrdU pulse experiments, one mg BrdU was injected intraperitoneally 24h prior to euthanization and subsequent organ harvest. After surface staining, intracellular BrdU staining was carried out according to the manufacturer's protocol.

**Cell cycle analysis.** Following surface staining, intracellular staining was performed as described previously<sup>10</sup>. To assess cell cycles, we stained for the nuclear antigen KI67 (eBioscience, clone SolA15) and DNA (4,6-diamidino-2-phenylindole, DAPI, FxCycle Violet Stain, Life Technologies).

**Cell sorting.** For sorting hematopoietic stem/progenitor cells, bone marrow was collected from WT mice by crushing bones from femurs, tibiae, humeri, pelvic bones and spines with a mortar and pestle. To enrich samples for hematopoietic stem/progenitor cells, we used MACS depletion columns (LD columns, Miltenyi) after incubation with a cocktail of biotin-labeled lineage antibodies (lineage for hematopoietic stem/progenitor staining as described above) followed by incubation with streptavidin-coated microbeads (Miltenyi). We then stained cells with c-kit, sca-1, CD48 and CD150 as described above and FACS-sorted LSKs and HSCs using a FACS Aria II cell sorter (BD Biosystems). To sort different hematopoietic stem cell niche populations, we utilized Nestin-GFP mice as described previously<sup>10</sup>. Cell suspensions were obtained from either flushed and digested bone marrow or crushed and digested bones. To

purify stromal niche cells from hematopoietic cells, we used MACS depletion columns (LD columns, Miltenyi) after incubation with biotin-labeled lineage antibodies (lineage for hematopoietic stem/progenitor staining as described above) followed by incubation with streptavidin-coated microbeads (Miltenyi). We subsequently stained with CD45.2, sca-1, CD31 (Biolegend, clone 390) and CD51 (Biolegend, clone RMV-7) and FACS-sorted stromal cells. Bone marrow endothelial cells (EC) were identified as  $lin^{low}$   $CD45^{low}$   $sca-1^{high}$   $CD31^{high}$ , bone marrow mesenchymal stromal cells (MSC) as  $lin^{low}$   $CD45^{low}$   $CD31^{low}$   $sca-1^{high/intermediate}$  and  $GFP^{+}$ , bone osteoblastic lineage cells (OB) as  $lin^{low}$   $CD45^{low}$   $sca-1^{low}$   $CD31^{low}$   $CD51^{high}$ . Many bone marrow stromal cells are also positive for the neurofilament protein Nestin<sup>11</sup> among them endothelial cells (EC), mesenchymal stromal cells (MSC) and osteoblastic cells (OBC). We used Nestin-GFP reporter mice for identifying MSC after we gated on cells that are  $CD45^{low}/CD31^{low}/sca-1^{high}$  and consequently excluded EC ( $CD31^{high}$ ) and OBC ( $sca-1^{low}$ ).

To sort heart macrophages, we harvested and digested 4d old infarcts (including their leukocyte-rich border zones) from WT mice. We subsequently stained for myeloid cells and FACS-sorted macrophages as described above.

**Bone marrow reconstitution assays.** We lethally irradiated WT or  $IL1R1^{-/-}$  mice with 950 cGy. We then reconstituted mice with  $2 \times 10^6$  whole bone marrow cells from either WT or  $IL1R1^{-/-}$  mice on the day of the irradiation. Two to four months later mice received coronary ligation, and respective experimental procedures were carried out.

**Fluorescence Molecular Tomography-Computed Tomography (FMT/CT).** We measured protease activity in hearts of  $ApoE^{-/-}$  mice 7d after MI by using fluorescence molecular tomography (FMT) in combination with computed tomography (CT) as described previously<sup>12</sup>. Pan-cathepsin protease sensor (Prosense-680, PerkinElmer, 5 nmol) was injected to evaluate inflammatory activity in infarcts.

**Histologic procedures.** For histological evaluations, WT mice were euthanized on day 7 after MI, and hearts were perfused thoroughly with PBS and then harvested. The hearts were embedded in O.C.T. compound (Sakura Finetek) and subsequently snap-frozen in a 2-methylbutane bath cooled with dry ice. For immunohistochemistry, 6  $\mu\text{m}$  frozen sections were stained using antibodies targeting CD11b (BD Biosciences, clone M1/70), Ly6G (Biolegend, clone 1A8), alpha-smooth muscle actin ( $\alpha\text{SMA}$ , Abcam, clone ab5694), collagen I (Abcam, clone ab21286) and CD31 (BD Biosciences, clone MEC13.3). The appropriate biotinylated secondary antibodies followed by VECTASTAIN ABC kit (Vector Laboratories, Inc.) were applied. We used an AEC substrate (Dako) for color development. All sections were counterstained with Harris hematoxylin. We scanned slides using a digital scanner, Nanozoomer 2.0RS (Hamamatsu, Japan), and quantified the positive area using IPLab (version 3.9.3; Scanalytics, Inc.). We analyzing five high-power fields per section and per animal.

**Quantitative real-time PCR.** Messenger RNA (mRNA) was extracted from 7d old infarcts (+border zones) or from flushed bone marrow, using the RNeasy Mini Kit (Qiagen), or from FACS-sorted cells, using the Arcturus PicoPure RNA Isolation Kit (Applied Biosystems), according to manufacturers' protocols. We transcribed one microgram of mRNA to complimentary DNA (cDNA) with the high capacity RNA to cDNA kit (Applied Biosystems). We used Taqman primers (Applied Biosystems) for the quantitative real-time PCR. We expressed the results as Ct values normalized to the housekeeping gene Gapdh (with the control set as 1).

**CFU-assay.** Colony forming unit (CFU) assays were performed, as recommended by the manufacturer, using a semi-solid cell culture medium (Methocult M3434, Stem Cell Technology). We flushed bones with Iscove's Modified Dulbecco's Medium (IMDM, Lonza) supplemented with 2% fetal calf serum. We plated  $2 \times 10^4$  bone marrow cells on a 35 mm plate in duplicates<sup>10</sup>. After incubating for 12 days, colonies were counted using a low magnification inverted microscope.

**Magnetic resonance imaging (MRI).** MRI was carried out on days 1 and 21 after permanent coronary ligation as described perviously<sup>13, 14</sup>. We obtained cine images of the left ventricular short axis by using a 7 Tesla horizontal bore Pharmascan (Bruker) and a custom-built mouse cardiac coil (Rapid Biomedical). Acquisition was done as described previously<sup>13</sup>. Images were analyzed using the software Segment (<http://segment.heiberg.se>).

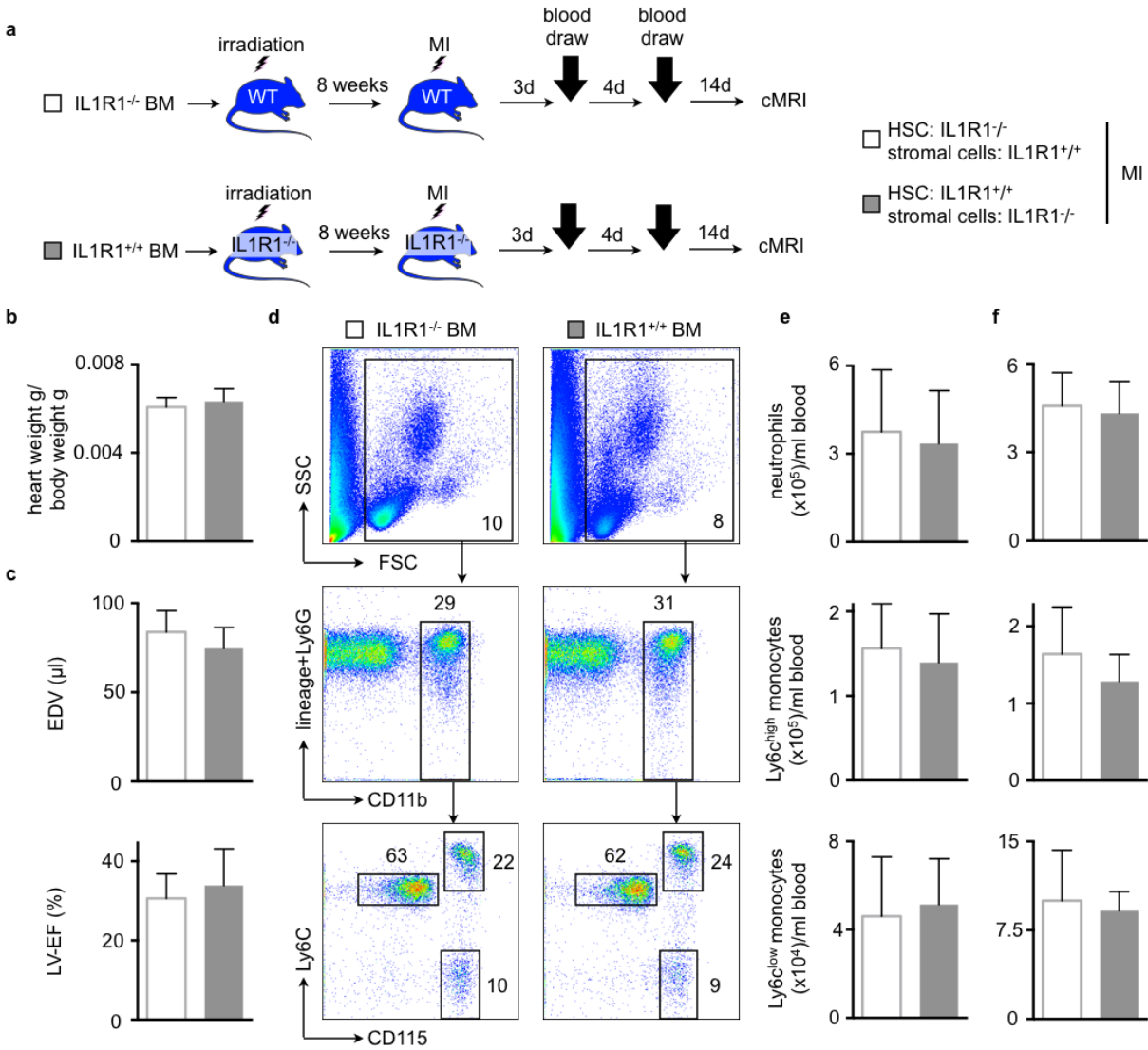
**IL-1 $\beta$  ELISA.** Blood was acquired by cardiac puncture and allowed to clot for 20 min at room temperature. After spinning down for 15 min at 2000 G, 50  $\mu$ l serum was used for further ELISA applications. Infarct and border zone parts were removed from heart samples and then snap frozen in liquid nitrogen. A mechanical tissue disruption was performed in 250  $\mu$ l RIPA lysis buffer (Millipore). After spinning down for 20 min at 12000 G, 5  $\mu$ l of the supernatant was used for further ELISA applications. For measuring protein levels of IL-1 $\beta$  in hearts and serum we used an ELISA kit (R&D Systems, MN, USA) according to the manufacturer's instructions.

**Administration of recombinant mouse IL-1 $\beta$ .** We injected 2.5  $\mu$ g of recombinant mouse IL-1 $\beta$  (R&D Systems, MN, USA) i.p. daily over two days as described elsewhere<sup>15</sup> and harvested the bone marrow 48h after the first administration.

**Statistics.** Statistical analyses were carried out using GraphPad Prism software version 6 (GraphPad Software, Inc.). Results are displayed as mean  $\pm$  standard deviation (SD). First, values were tested for Gaussian distribution (D'Agostino-Pearson omnibus normality test). For two-group comparisons, an unpaired t-test was applied to normally distributed variables, a Mann-Whitney test to non-normally distributed variables. For comparing more than two groups, a one-way ANOVA test, followed by a Sidak's test for multiple comparisons, was applied. P values of < 0.05 indicated statistical significance.

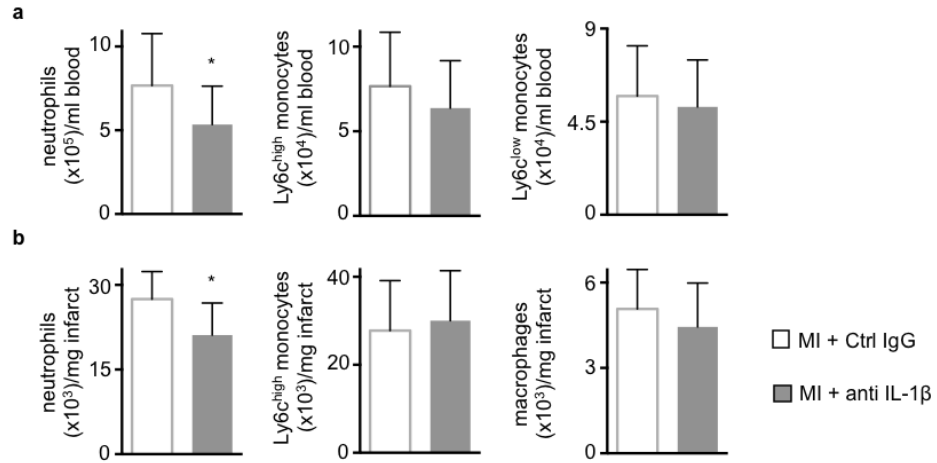


## Supplemental Figures and Figure Legends



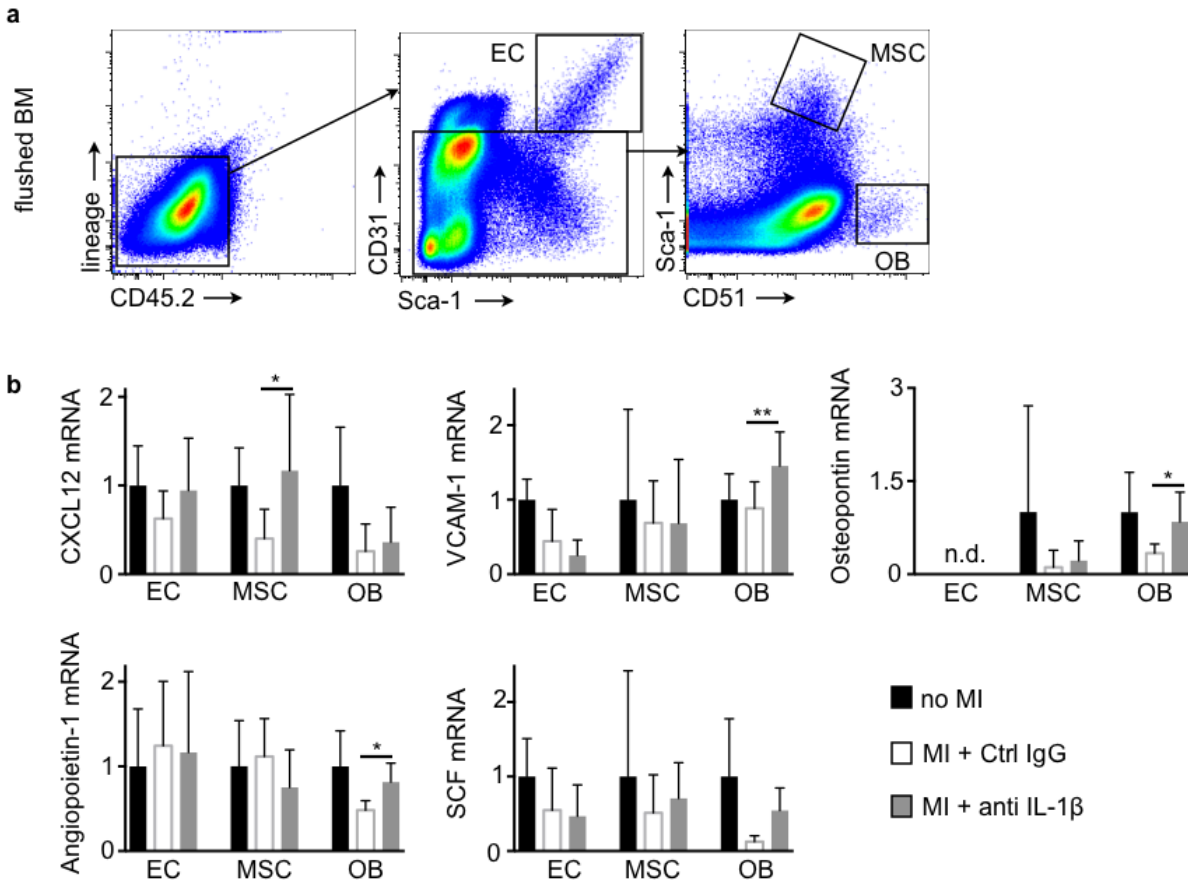
### Supplemental Figure 1. IL-1 $\beta$ drives HSC proliferation both directly and indirectly.

**(a)** Experimental set-up of the BM reconstitution experiment. Lethally irradiated wild type (WT) or IL1R1<sup>-/-</sup> mice were reconstituted with IL1R1<sup>-/-</sup> or WT bone marrow, respectively. Eight weeks later, mice received MI and were subjected to the described procedures. **(b)** Quantification of heart to total body weight 21d after coronary ligation (n = 8-10 per group, mean  $\pm$  SD). **(c)** Evaluation of post-MI remodeling by cardiac MRI. End-diastolic volumes (EDV) and left-ventricular ejection fraction (LV-EF) were examined on day 21 after coronary ligation (n = 8-10 per group, mean  $\pm$  SD). **(d)** Flow cytometric gating for blood leukocyte subsets 7 d after coronary ligation. **(e,f)** Quantification of blood leukocyte numbers 3 d **(e)** and 7 d **(f)** after coronary ligation (n = 10-12 per group, mean  $\pm$  SD).

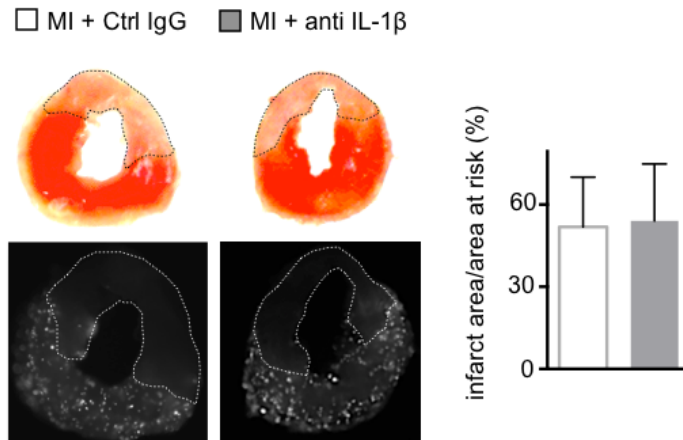


**Supplemental Figure 2. IL-1 $\beta$  effects on day 3 after MI.**

(a,b) Flow cytometric quantification of (a) blood and (b) heart neutrophils and monocytes/macrophages 3d after coronary ligation (n = 13-14 per group, mean  $\pm$  SD, \*p<0.05).



**Supplemental Figure 3. Neutralizing IL-1 $\beta$  changes the bone marrow microenvironment.** (a) Flow cytometric gating for sorting respective bone marrow (BM) stromal cell populations (EC, bone marrow endothelial cells; MSC, bone marrow mesenchymal stromal cells; OB, bone osteoblastic lineage cells). (b) mRNA quantification of HSC retention factors (CXCL12, chemokine (C-X-C motif) ligand 12, VCAM-1, vascular cell adhesion molecule 1; SCF, stem cell factor and OPN, osteopontin) in respective BM stromal cells with qRT-PCR 48h after MI (n = 7-8 per group, mean  $\pm$  SD, \* $p$ <0.05, \*\* $p$ <0.01).



**Supplemental Figure 4. Anti-IL-1 $\beta$  treatment does not alter the infarct size in ischemia reperfusion injury.**

Quantification of the infarct area (upper panel, dashed line shows TTC negative area) to the area at risk (lower panel, dashed line shows area spared from fluorescent microspheres as assessed with fluorescence reflectance imaging) 24 h after 35 min of ischemia. Percent infarction over area at risk is calculated as TTC-negative area / FRI-negative area \* 100% (n = 5-7 per group, mean  $\pm$  SD).

## Supplemental References

1. Encinas JM, Michurina TV, Peunova N, Park JH, Tordo J, Peterson DA, Fishell G, Koulakov A, Enikolopov G. Division-coupled astrocytic differentiation and age-related depletion of neural stem cells in the adult hippocampus. *Cell Stem Cell*. 2011; 8:566-579.
2. Mignone JL, Kukekov V, Chiang AS, Steindler D, Enikolopov G. Neural stem and progenitor cells in nestin-GFP transgenic mice. *J Comp Neurol*. 2004; 469:311-324.
3. Dutta P, Courties G, Wei Y, Leuschner F, Gorbатов R, Robbins CS, Iwamoto Y, Thompson B, Carlson AL, Heidt T, Majmudar MD, Lasitschka F, Etzrodt M, Waterman P, Waring MT, Chicoine AT, van der Laan AM, Niessen HW, Piek JJ, Rubin BB, Butany J, Stone JR, Katus HA, Murphy SA, Morrow DA, Sabatine MS, Vinegoni C, Moskowitz MA, Pittet MJ, Libby P, Lin CP, Swirski FK, Weissleder R, Nahrendorf M. Myocardial infarction accelerates atherosclerosis. *Nature*. 2012; 487:325-329.
4. Leuschner F, Dutta P, Gorbатов R, Novobrantseva TI, Donahoe JS, Courties G, Lee KM, Kim JI, Markmann JF, Marinelli B, Panizzi P, Lee WW, Iwamoto Y, Milstein S, Epstein-Barash H, Cantley W, Wong J, Cortez-Retamozo V, Newton A, Love K, Libby P, Pittet MJ, Swirski FK, Koteliansky V, Langer R, Weissleder R, Anderson DG, Nahrendorf M. Therapeutic siRNA silencing in inflammatory monocytes in mice. *Nat Biotechnol*. 2011; 29:1005-1010.
5. Robbins CS, Hilgendorf I, Weber GF, Theurl I, Iwamoto Y, Figueiredo JL, Gorbатов R, Sukhova GK, Gerhardt LM, Smyth D, Zavitz CC, Shikatani EA, Parsons M, van Rooijen N, Lin HY, Husain M, Libby P, Nahrendorf M, Weissleder R, Swirski FK. Local proliferation dominates lesional macrophage accumulation in atherosclerosis. *Nat Med*. 2013; 19:1166-1172.
6. Geiger T, Towbin H, Cosenti-Vargas A, Zingel O, Arnold J, Rordorf C, Glatt M, Vosbeck K. Neutralization of interleukin-1 beta activity in vivo with a monoclonal antibody alleviates collagen-induced arthritis in DBA/1 mice and prevents the associated acute-phase response. *Clin Exp Rheumatol*. 1993; 11:515-522.

7. Osborn O, Brownell SE, Sanchez-Alavez M, Salomon D, Gram H, Bartfai T. Treatment with an Interleukin 1 beta antibody improves glycemic control in diet-induced obesity. *Cytokine*. 2008; 44:141-148.
8. Nahrendorf M, Swirski FK, Aikawa E, Stangenberg L, Wurdinger T, Figueiredo JL, Libby P, Weissleder R, Pittet MJ. The healing myocardium sequentially mobilizes two monocyte subsets with divergent and complementary functions. *J Exp Med*. 2007; 204:3037-3047.
9. Swirski FK, Libby P, Aikawa E, Alcaide P, Luscinskas FW, Weissleder R, Pittet MJ. Ly-6Chi monocytes dominate hypercholesterolemia-associated monocytosis and give rise to macrophages in atheromata. *J Clin Invest*. 2007; 117:195-205.
10. Heidt T, Sager HB, Courties G, Dutta P, Iwamoto Y, Zaltsman A, von Zur Muhlen C, Bode C, Fricchione GL, Denninger J, Lin CP, Vinegoni C, Libby P, Swirski FK, Weissleder R, Nahrendorf M. Chronic variable stress activates hematopoietic stem cells. *Nat Med*. 2014; 20:754-758.
11. Schepers K, Pietras EM, Reynaud D, Flach J, Binnewies M, Garg T, Wagers AJ, Hsiao EC, Passegue E. Myeloproliferative neoplasia remodels the endosteal bone marrow niche into a self-reinforcing leukemic niche. *Cell Stem Cell*. 2013; 13:285-299.
12. Nahrendorf M, Waterman P, Thurber G, Groves K, Rajopadhye M, Panizzi P, Marinelli B, Aikawa E, Pittet MJ, Swirski FK, Weissleder R. Hybrid in vivo FMT-CT imaging of protease activity in atherosclerosis with customized nanosensors. *Arterioscler Thromb Vasc Biol*. 2009; 29:1444-1451.
13. Courties G, Heidt T, Sebas M, Iwamoto Y, Jeon D, Truelove J, Tricot B, Wojtkiewicz G, Dutta P, Sager HB, Borodovsky A, Novobrantseva T, Klebanov B, Fitzgerald K, Anderson DG, Libby P, Swirski FK, Weissleder R, Nahrendorf M. In Vivo Silencing of the Transcription Factor IRF5 Reprograms the Macrophage Phenotype and Improves Infarct Healing. *J Am Coll Cardiol*. 2014; 63:1556-1566.
14. Majmudar MD, Keliher EJ, Heidt T, Leuschner F, Truelove J, Sena BF, Gorbатов R, Iwamoto Y, Dutta P, Wojtkiewicz G, Courties G, Sebas M, Borodovsky A, Fitzgerald K,

Nolte MW, Dickneite G, Chen JW, Anderson DG, Swirski FK, Weissleder R, Nahrendorf M. Monocyte-directed RNAi targeting CCR2 improves infarct healing in atherosclerosis-prone mice. *Circulation*. 2013; 127:2038-2046.

15. Chou RC, Kim ND, Sadik CD, Seung E, Lan Y, Byrne MH, Haribabu B, Iwakura Y, Luster AD. Lipid-cytokine-chemokine cascade drives neutrophil recruitment in a murine model of inflammatory arthritis. *Immunity*. 2010; 33:266-278.